

Supplementary Information

First identification of unstable phosphino formic acid (H_2PCOOH)

*Cheng Zhu,^a Robert Frigge,^a Andrew M. Turner,^a Ralf I. Kaiser,^{*a} Bing-Jian Sun,^b*

Si-Ying Chen^b and Agnes H.H. Chang^b

^aDepartment of Chemistry, University of Hawaii at Mānoa, Honolulu, HI 96822

W.M. Keck Laboratory in Astrochemistry, University of Hawaii at Mānoa, Honolulu, HI 96822

^bDepartment of Chemistry, National Dong Hwa University, Shoufeng, Hualien 974, Taiwan

Corresponding Author

*E-mail: ralfk@hawaii.edu

Content:

Materials & Methods – Experimental

Materials & Methods – Theoretical

Fig. S1

Table S1 to S5

Materials & Methods – Experimental

The experiments were conducted in a contamination-free ultrahigh vacuum chamber with a base pressure 8×10^{-11} Torr, which was rendered using a magnetically suspended turbo molecular pump (Osaka TG420 MCAB) backed by an oil-free scroll pump (Anest Iwata ISP-500).¹ Within the chamber, a silver mirror substrate is interfaced to a cold head (Sumitomo Heavy Industries, RDK-415E), which is connected to a closed cycle helium compressor capable of reaching 5.0 ± 0.1 K. By utilizing a doubly differentially pumped rotational feedthrough (Thermionics Vacuum Products, RNN-600/FA/ MCO) the substrate is able to be rotated in the horizontal plane; utilizing an UHV compatible bellow (McAllister, BLT106) the substrate can be translated in the vertical plane as well. The gas mixture was prepared in a gas mixing chamber by the sequential addition of 10 mbar of phosphine (PH_3 , Sigma-Aldrich, 99.9995%;) and 100 mbar of carbon dioxide (CO_2 , Airgas, 99.999%;¹³ CO_2 , Aldrich, 99% ¹³C; ¹⁸ O_2 , Aldrich, 95% ¹⁸O). The premixed gases were then deposited to the silver wafer at 5 K via a precision leak valve and glass capillary array for 15 min at a pressure of 2×10^{-8} Torr in the main chamber. The thickness of the ice was determined in situ via laser interferometry with one helium-neon (He-Ne) laser operating at 632.8 nm.² The light from the laser was reflected at angles of 4° relative to the ice surface normal. Considering the ratio of phosphine (PH_3) and carbon dioxide (CO_2) (1:10; see below) and the refractive indexes of pure phosphine (PH_3 , $n_{\text{PH}_3} = 1.51 \pm 0.04$) and carbon dioxide ($n_{\text{CO}_2} = 1.27 \pm 0.02$) ices^{2,3}, the ice thickness was determined to 830 ± 50 nm.

The deposited ice was then monitored via a Fourier Transform Infrared (FTIR) spectrometer (Nicolet 6700) from 6,000–500 cm⁻¹ and a resolution of 4 cm⁻¹. Fig. S1(a) depicts the IR spectrum of phosphine (PH_3) and carbon dioxide (CO_2) ice. Vibrational assignments were compiled in Table S1. Based on the integrated areas along with absorption coefficients of 1.40×10^{-18} cm molecule⁻¹, 4.50×10^{-19} cm molecule⁻¹, 7.80×10^{-17} cm molecule⁻¹, 7.1×10^{-19} cm molecule⁻¹, and 5.1×10^{-19} cm molecule⁻¹ for the 3699 cm^{-1} ($v_1 + v_3$, CO_2), 3594 cm^{-1} ($2v_2 + v_3$, CO_2), 2274 cm^{-1} (v_3 , ¹³ CO_2), 1103 cm^{-1} (v_4 , PH_3), and 987 cm^{-1} (v_2 , PH_3) bands, respectively, the relative abundance of phosphine (PH_3) and carbon dioxide (CO_2) was determined to be nominally 1:10,^{2,3} which matches the gas phase ratio. Furthermore, the absorptions of carbon dioxide (CO_2) at 3699 cm^{-1} ($v_1 + v_3$) and 3594 cm^{-1} ($2v_2 + v_3$) are red shifted from that of pure carbon dioxide (CO_2) ice (Fig. S1(b)), which probably due to the complexation effect of carbon

dioxide (CO_2) and phosphine (PH_3), e.g., redistribution of the partial atomic charges and change of the bond orders.

The ices were then isothermally irradiated at 5.0 ± 0.1 K with 5 keV electrons from a Specs EQ 22-35 electron gun at nominal beam current of 0 nA (blank), 100 nA. The electrons were introduced at an angle of 70° relative to the target surface and expanded to cover the ice area (1.0 ± 0.1 cm^2). Monte Carlo simulations (Casino 2.42)⁴ were exploited to model the electron trajectories and energy transfer inside the ices. Considering the densities of phosphine (PH_3 , 0.90 g cm^{-3})² and carbon dioxide (CO_2 , 1.11 g cm^{-3})³ the average and maximum penetration depths of the 5 keV electrons were calculated to be 300 ± 40 and 700 ± 80 nm, respectively, which are less than the thickness of the deposited ice mixtures of 830 ± 50 nm ensuring negligible interaction between the substrate and the electrons. The averaged dose was calculated to be 2.8 ± 0.6 per molecule. During the irradiation, IR spectra of the ices were continuously measured every 2 minutes. New absorptions at 2284 cm^{-1} (P_2H_4),² 2137 cm^{-1} (CO , 2137 cm^{-1}),³ and 2092 cm^{-1} (^{13}CO)³ were identified in the IR spectrum of the 100 nA irradiated phosphine (PH_3) and carbon dioxide (CO_2) ice. The most intense absorptions of phosphino formic acid (H_2PCOOH), e.g., 1101, 1131, and 1790 cm^{-1} , were not found in the spectrum since FTIR is relatively insensitive compared to PI-ReTOF-MS by at least four orders of magnitude,⁵ and the present low dose experiment was designed to initiate only the initial reactions in the carbon dioxide – phosphine ices and hence to exclude the formation of higher phosphanes.

After the irradiation, the ices were heated at a rate of 1 K min^{-1} to 320 K while any subliming molecules were detected using a reflectron time-of-flight (ReTOF) mass spectrometer (Jordon TOF Products, Inc.) with single photon ionization.¹ This photoionization process utilizes difference four wave mixing to produce vacuum ultraviolet light ($\omega_{\text{vuv}} = 2\omega_1 - \omega_2$). The experiments were performed with 10.86 eV photoionization energy and repeated at 9.60 eV to distinguish between the isomers of the phosphino formic acid (H_2PCOOH). To produce 10.86 eV, the second harmonic (532 nm) of a pulsed neodymium-doped yttrium aluminum garnet laser (Nd:YAG, Spectra Physics, PRO-270, 30 Hz) was used to pump a Rhodamine 610/640 dye mixture ($0.17/0.04 \text{ g L}^{-1}$ ethanol) to obtain 606.9 nm (2.04 eV) (Sirah, Cobra-Stretch), which underwent a frequency tripling process to achieve $\omega_1 = 202.3 \text{ nm}$ (6.13 eV) ($\beta\text{-BaB}_2\text{O}_4$ (BBO) crystals, 44° and 77°). A second Nd:YAG laser pumped an LDS 867 (0.15 g L^{-1} ethanol) dye to obtain $\omega_2 = 890 \text{ nm}$ (1.39 eV), which when combined with $2\omega_1$, using krypton as a non-linear

medium, generated $\omega_{\text{vuv}} = 114.2 \text{ nm}$ (10.86 eV) at 10^{14} photons per pulse. The production of 9.60 eV occurred similarly except the third harmonic (355 nm) of the second Nd:YAG laser was used to pump a Coumarin 480 (0.40 g L⁻¹ ethanol) dye to obtain $\omega_2 = 472.1 \text{ nm}$ (2.63 eV). The VUV light was spatially separated from other wavelengths (due to multiple resonant and non-resonant processes ($2\omega_1 + \omega_2$; $2\omega_1 - \omega_2$; $3\omega_1$; $3\omega_2$)) using a lithium fluoride (LiF) biconvex lens (ISP Optics) and directed 2 mm above the sample to ionize subliming molecules. The ionized molecules were mass analyzed with the ReTOF mass spectrometer where the arrival time to a multichannel plate is based on mass-to-charge ratios, and the signal was amplified with a fast preamplifier (Ortec 9305) and recorded with a personal computer multichannel scalar (FAST ComTec, P7888-1 E), which is triggered via the pulse delay generator at 30 Hz. Here the ReTOF signal is the average of 3600 sweeps of the mass spectrum in 4 ns bin widths, which corresponds to an increase in the substrate temperature of 2 K between the ReTOF data points.

Materials and Methods – Theoretical

The geometries of phosphino formic acid (H₂PCOOH) and carbamic acid (H₂NCOOH) isomers are optimized by the hybrid density functional B3LYP⁶⁻⁹ with the cc-pVTZ basis set and the harmonic frequencies obtained (Tables S2 and S3). The corresponding coupled cluster¹⁰⁻¹³ CCSD(T)/cc-pVDZ, CCSD(T)/ccpVTZ, and CCSD(T)/cc-pVQZ energies are calculated and extrapolated to completed basis set limits,¹⁴ CCSD(T)/CBS, with B3LYP/cc-pVTZ zero-point energy corrections. Likewise, the species along the phosphino formic acid (H₂PCOOH) and carbamic acid (H₂NCOOH) decomposition pathways are predicted at the same level of theory (Tables S4 and S5). The energies are expected to be accurate within 0.08 eV.¹⁵ The adiabatic ionization energies are computed by taking the energy difference between the neutral and ionic species that correspond to similar conformation. The adiabatic ionization energies at this level of calculations (B3LYP/cc-pVTZ//CCSD(T)/CBS) are expected to be accurate within ± 0.05 eV.¹⁶ The GAUSSIAN09 program¹⁷ was utilized in the electronic structure calculations.

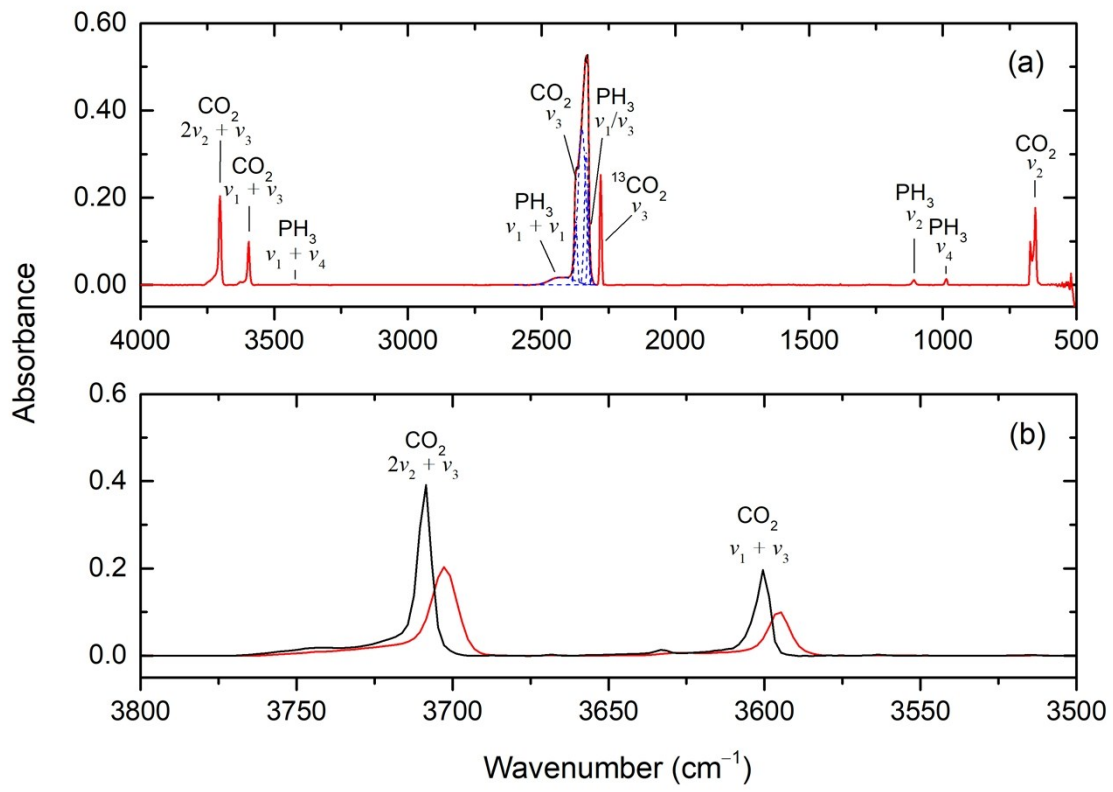


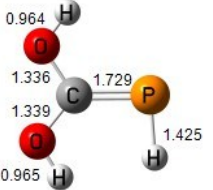
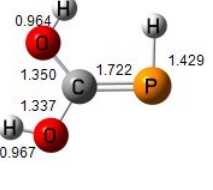
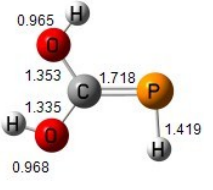
Fig. S1. (a) Infrared spectrum of phosphine (PH_3) – carbon dioxide (CO_2) ice. The absorption features in the range of $2500 - 2290 \text{ cm}^{-1}$ are deconvoluted with Gaussian functions (dash lines). (b) Infrared spectra in the range of $3800 - 3500 \text{ cm}^{-1}$ of phosphine (PH_3) – carbon dioxide ice (CO_2) (red) and pure carbon dioxide (CO_2) ice (black).

Table S1. Absorption peaks observed in pristine phosphine (PH_3) – carbon dioxide (CO_2) ice.

Assignment	Wavenumber (cm^{-1})
$\text{CO}_2 (\nu_2)$	665 ³
$\text{PH}_3 (\nu_2)$	987 ²
$\text{PH}_3 (\nu_4)$	1103 ²
$^{13}\text{CO}_2 (\nu_3)$	2274 ³
$\text{PH}_3(\nu_1/\nu_3)$	2326 ²
$\text{CO}_2 (\nu_3)$	2372-2333 ³
$\text{PH}_3(\nu_1 + \nu_3)$	2423 ²
$\text{PH}_3 (\nu_1 + \nu_4)$	3410 ²
$\text{CO}_2 (2\nu_2 + \nu_3)$	3587 ³
$\text{CO}_2 (\nu_1 + \nu_3)$	3695 ³

Table S2: Computed Cartesian coordinates (\AA), vibrational frequencies (cm^{-1}), and IR intensities (km mol^{-1}) for various isomers of phosphino formic acid (H_2PCOOH).

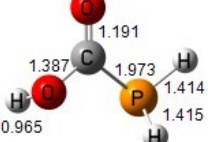
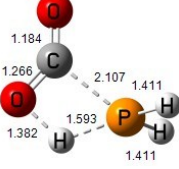
Name and formula	#	Structure	Cartesian coordinate ^a				Vibrational frequency	IR intensities
			Atom	X	Y	Z		
Phosphino formic acid (H_2PCOOH)	1a		P	1.339853	-0.040703	-0.118564	157.69 297.6187 427.3112 492.8792 655.8341 695.2596 826.3971 851.3929 1101.9474 1130.9682 1315.9839 1790.1092 2414.0172 2429.849 3701.5389	4.2926 2.3065 9.146 27.2694 106.5977 52.549 44.7314 3.0997 136.1168 166.3544 23.2594 323.3449 30.2534 35.7818 52.6963
			H	1.607026	1.018713	0.780168		
			H	1.476858	-1.072409	0.842620		
			C	-0.520039	0.131164	0.012837		
			O	-1.114431	1.174103	0.006292		
			O	-1.132180	-1.075951	0.005224		
			H	-2.088548	-0.907952	-0.013483		
	1b		P	-1.326274	0.022015	-0.119931	128.0346 306.4442 410.3684 441.1907 566.6445 716.9487 815.6209 841.7435 1098.2947 1131.8298 1268.3074 1828.9819 2370.1996 2435.2855 3795.251	6.6371 8.0283 24.7411 66.5405 3.9107 19.8133 31.3429 7.2021 83.008 27.9451 386.2515 289.6837 55.6275 23.9218 44.5835
			H	-1.583164	-0.964407	0.859802		
			H	-1.475066	1.115659	0.777315		
			C	0.551832	-0.136740	0.012026		
			O	1.100186	-1.197174	0.006242		
			O	1.269042	1.016464	-0.000045		
			H	0.687523	1.784648	0.040118		
			P	-0.081604	-1.359646	0.000000	326.3528 357.7777 480.8702 519.8393 540.3575	6.9888 22.3577 2.9216 58.9443 123.6528
			H	1.334325	-1.520806	0.000000		

	2a		C	0.000000	0.367115	0.000000	753.6866 916.4721 1141.9027 1169.1021 1408.2523 1446.081 2346.2391 3795.9623 3815.2421	5.873 41.2244 70.6278 359.1156 51.5304 549.8491 93.5439 86.5733 68.5687
Enol tautomer (HPC(OH) ₂)	2b		P	-0.198350	-1.373419	0.000000	293.5013 358.3573 476.4882 479.6489 527.8369 605.5234 740.6149 937.3438 1106.8269 1184.6692 1364.6015 1477.8233 2325.6545 3761.6917 3800.7153	126.0207 2.0995 13.9618 8.3026 65.9094 0.5738 17.7659 63.9698 276.2262 175.9576 152.4949 347.4136 113.8864 126.6074 65.2495
			H	1.213010	-1.594405	0.000000		
			C	0.000000	0.336801	0.000000		
			O	-1.062194	1.148317	0.000000		
			H	-0.757156	2.065852	0.000000		
			O	1.140472	1.058336	0.000000		
			H	1.893179	0.455804	0.000000		
	2c		P	-0.020432	-1.382416	0.000000	318.5421 346.9201 451.7892 476.7941 536.4282 611.3931 741.8152 884.3131 1107.2307 1191.4377 1363.6952 1484.6537 2394.603 3737.4799 3786.4297	176.6647 6.0975 6.274 15.5225 37.2585 2.2129 14.2532 29.8335 270.8496 188.0745 141.0895 350.2741 49.3774 100.5161 71.8439
			H	-1.437673	-1.454663	0.000000		
			C	0.000000	0.335539	0.000000		
			O	1.139462	1.064353	0.000000		
			H	1.903361	0.474547	0.000000		
			O	-1.064137	1.140941	0.000000		
			H	-0.761801	2.060774	0.000000		

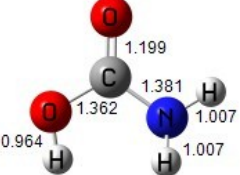
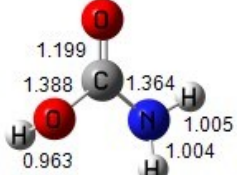
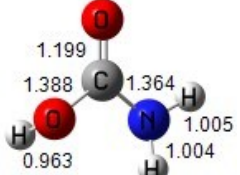
			P	1.388121	-0.099688	0.009688	270.8385	152.8459
			H	1.550885	1.307770	-0.114864	352.8225	13.2484
			C	-0.313362	0.004870	-0.002833	461.276	166.6911
			O	-1.062761	-1.126646	-0.068450	474.6655	10.3595
			H	-1.834621	-1.044616	0.508800	532.5159	6.5047
			O	-1.035528	1.148497	0.055324	571.4574	12.2261
			H	-1.871596	1.028144	-0.417238	738.5969	0.0416
			P	1.357968	-0.164726	0.000000	905.4752	51.4839
			H	0.943571	-1.065508	1.021791	1106.5761	308.515
			H	0.943571	-1.065508	-1.021791	1198.3938	7.5758
			O	0.000000	0.871204	0.000000	1266.2607	299.9969
			O	-1.586940	-0.751361	0.000000	1463.063	123.6869
			C	-1.266294	0.399399	0.000000	2377.9188	64.2797
			H	-1.963379	1.246760	0.000000	3724.1431	33.9013
			P	-1.257685	-0.257608	-0.116436	3734.3953	61.083
			H	-1.130218	-0.887665	1.153461	153.9445	6.4368
			H	-2.205493	0.686580	0.361569	225.2565	10.8258
			O	0.033907	0.879044	0.037089	275.55	17.4593
			O	1.536103	-0.798069	-0.009759	662.8877	57.875
							736.4491	13.5722
							910.5112	14.8619

			C	1.271790	0.372332	0.002601	2365.7803	62.1742
			H	2.010158	1.183422	-0.002726	2388.5949	76.7112
Formic phosphinous anhydride (HCOOPH ₂)	3c		P	1.535719	-0.162292	0.000000	74.7345	2.7907
			H	1.345918	-1.135158	1.027683	128.0608	4.4296
			H	1.345918	-1.135158	-1.027683	263.677	1.2665
			O	0.000000	0.541274	0.000000	512.6377	26.7263
			O	-2.226302	0.338121	0.000000	850.4533	109.2847
			C	-1.155577	-0.177300	0.000000	916.6315	14.263
			H	-0.983738	-1.266666	0.000000	975.4988	48.0305
							1036.7987	1.0314
	3d		P	-1.451960	-0.378561	0.000000	120.7747	0.6236
			H	-2.086112	0.365550	1.030279	162.6008	17.4389
			H	-2.086112	0.365550	-1.030279	268.3894	0.882
			O	0.000000	0.507925	0.000000	513.6433	29.4408
			O	2.228880	0.392587	0.000000	854.7161	137.7817
			C	1.178286	-0.165926	0.000000	893.1981	45.7097
			H	1.050872	-1.261216	0.000000	905.3891	9.2051
							1043.5126	0.0149

Table S3: Computed cartesian coordinates (Å), vibrational frequencies (cm⁻¹), and IR intensities (km mol⁻¹) for the species related to the decomposition of phosphino formic acid (H₂PCOOH) and carbamic acid (H₂NCOOH).

Name and notation	Structure	Cartesian coordinatea				Vibrational frequency	IR intensities
		Atom	X	Y	Z		
P-Transition state1		C	-0.530773	0.162411	0.016685	-558.4678	98.2194
		O	-1.091209	1.213331	-0.000882	181.9724	9.0882
		P	1.322176	-0.076747	-0.11635	294.7046	3.0362
		H	1.680347	1.132693	0.523835	424.9858	0.7555
		H	1.445164	-0.89945	1.028789	504.5199	33.4002
		O	-1.211627	-1.042122	0.10817	728.1703	17.5277
		H	-1.350821	-1.426181	-0.765799	804.6748	49.1781
						819.4281	21.7518
P-Transition state 2		C	0.000000	0.808781	0.000000	-1569.8479	750.808
		O	-0.851089	1.631209	0.000000	108.5644	0.3593
		P	-0.195740	-1.289085	0.000000	214.0492	88.5358
		H	-0.813159	-1.933078	1.092627	386.9166	2.9281
		H	-0.813159	-1.933078	-1.092627	461.8801	54.8904
		O	1.263982	0.742500	0.000000	683.5734	316.6229
		H	1.259269	-0.639924	0.000000	699.4035	3.2541
		C	-1.758337	-0.021397	-0.000069	748.107	89.0436
		O	-1.657277	-1.177549	-0.000005	1043.1299	0.3075

PH ₃ and CO ₂ complex		P	2.029748	0.046623	-0.000703	98.6953 663.5305 672.6549 1017.5423 1136.7568 1137.1795 1371.5125 2392.0179 2399.4369 2401.7981 2416.2312	1.6146 52.1003 27.7629 26.8649 9.056 9.9865 0.0366 38.0982 13.0294 56.9558 606.2279
		H	2.689860	-0.642734	1.050804		
		H	2.696063	-0.682919	-1.020710		
		O	-1.874149	1.132979	-0.000070		
		H	2.969279	1.111242	-0.018542		
Phosphine (PH ₃)		P	0.000000	0.000000	0.128193		
		H	0.000000	1.194495	-0.640964	1017.2772 1137.5726 1137.5726 2386.2849	19.8767 11.0863 11.0868 34.8311
		H	1.034463	-0.597247	-0.640964	2394.3614 2394.3618	67.427 67.4207
		H	-1.034463	-0.597247	-0.640964		
Carbon dioxide (CO ₂)		C	0.000000	0.000000	0.000000		
		O	0.000000	0.000000	1.160338	671.7935 671.7935 1371.8079	31.8622 31.8622 0
		O	0.000000	0.000000	-1.160338	2417.0441	629.3311
Carbamic acid a		C	-0.037006	0.125500	-0.001350	199.1585 471.9527 494.1470 579.9022 588.5957 784.2446 951.0780 1080.3233 1230.3628 1425.4610 1617.4536 1830.6590 3617.4267	218.9588 38.9184 22.3049 52.1434 43.9553 28.2643 45.4304 60.3494 186.9924 126.8979 107.6253 506.7886 48.9341
		O	-0.449442	1.261103	0.004017		
		H	1.958089	0.470159	0.086017		
		H	1.524724	-1.207238	0.099975		
		O	-0.848331	-0.968827	0.001643		
		H	-1.750996	-0.626480	0.004210	3748.2096 3794.5707	59.8445 83.0179

		N	1.267485	-0.246806	-0.032483		
Carbamic acid b		C	0.051288	-0.152712	0.001517	341.3114 440.4958 517.3185 556.0152 610.8336 775.2903 936.9562 1083.3064 1235.9149 1359.7292 1638.4967 1859.7188 3569.5566 3679.4977 3804.8842	64.4970 151.8760 14.6075 120.1957 17.6239 28.6498 47.3274 12.4414 41.0776 395.8842 63.9309 425.7012 25.6685 31.6899 40.2748
		O	0.265864	-1.332549	0.007134		
		H	-1.954612	-0.249845	0.059222		
		H	-1.364511	1.307747	0.366927		
		O	1.072005	0.749392	0.021832		
		H	0.758864	1.633417	-0.199189		
		N	-1.207203	0.412886	-0.066827		
N-Transition state 1		C	0.007256	0.159628	-0.006990	-464.7408 413.8169 497.0835 567.9784 611.2456 718.5407 909.0529 1115.6288 1184.0009 1325.3391 1617.2558 1841.7922 3592 3718.0934 3818.2022	91.6562 230.8078 1.8132 24.1011 10.3353 34.9552 72.4306 21.5935 121.6527 217.196 87.7414 467.4689 35.9433 44.4244 81.0914
		O	0.033637	1.358766	0.005407		
		H	-2.001208	-0.126241	-0.041248		
		H	-1.073440	-1.566425	-0.228230		
		O	1.151580	-0.619711	-0.107128		
		H	1.398185	-0.953734	0.762022		
		N	-1.121258	-0.603401	0.051881		
N-T transition		C	-0.311573	0.025927	-0.000002	-1731.7936 331.8869 451.5007 592.2783 767.8410 785.0494 983.0111	997.5140 6.0727 15.6513 2.1347 346.5769 10.5982 51.7302
		O	-1.290886	-0.647867	-0.000001		
		H	1.411533	-1.070720	0.828749		
						1027.7460 5.1000	

		H	1.411567	-1.070634	-0.828789	1387.2900 1565.9155 1891.1894 2151.6866 3480.8833 3579.7292	48.4642 64.1295 638.7190 6.2968 17.6626 33.8990
		C	0.943817	-0.000377	0.000203	13.6261 62.9738 100.0007 158.6617 205.0578 643.7116 677.1851 1066.5584 1369.5837 1671.8821 1672.6970 2413.5964 3465.7942 3582.4634 3584.9789	0.1466 15.2775 0.8400 45.5339 22.0523 66.4127 31.6321 132.5459 1.0296 18.1683 18.7915 599.6038 0.5213 2.7641 3.2717
NH ₃ and CO ₂ complex		O	0.977312	1.159826	0.000085		
		H	-2.402003	0.487207	0.800660		
		H	-2.389209	0.453268	-0.824981		
		O	0.973082	-1.160753	0.000078		
		H	-2.384439	-0.941262	0.017230		
		N	-2.012914	0.001495	0.000653		
Ammonia (NH ₃)		N	0.000000	0.000000	0.115439	1063.2493 1676.1802 1676.1806 3465.0403 3581.5498 3581.5501	147.4976 16.9120 16.9120 2.3635 0.5675 0.5673
		H	0.000000	0.937566	-0.269357		
		H	0.811956	-0.468783	-0.269357		
		H	-0.811956	-0.468783	-0.269357		

Table S4: Computed energies for various isomers of phosphino formic acid (H_2PCOOH).

Species	#	B3LYP/cc-pVTZ ^a (CCSD/cc-pVTZ ^{a'})	E_{zpc}^{b} ($E_{zpc}^{\text{b}'}$)	CCSD(T)/CBS ^c (CCSD(T)/CBS ^{c'})	IE(eV) ^d (IE(eV) ^{d'})	$E(\text{eV})^{\text{e}}$ ($E(\text{eV})^{\text{e}'}$)
Phosphino formic acid (H_2PCOOH)	1a	-531.779440 (-530.925802)	0.041665 (0.042656)	-531.120540 (-531.120665)	9.75 (9.74)	0.00 (0.00)
	1b	-531.771748 (-530.917714)	0.041360 (0.042377)	-531.112984 (-531.113136)	9.74 (9.73)	0.20 (0.20)
Enol tautomer (HPC(OH)_2)	2a	-531.746462 (-530.893148)	0.044725 (0.045718)	-531.092480 (-531.092602)	8.42 (8.43)	0.85 (0.85)
	2b	-531.746414 (-530.89293)	0.044291 (0.045314)	-531.091851 (-531.091976)	8.30 (8.31)	0.85 (0.85)
	2c	-531.746576 (-530.893015)	0.044273 (0.045308)	-531.091733 (-531.091869)	8.29 (8.29)	0.85 (0.86)
	2d	-531.737190 (-530.883906)	0.043692 (0.044795)	-531.082305 (-531.082462)	8.23 (8.23)	1.10 (1.10)
Formic phosphinous anhydride (HCOOPH_2)	3a	-531.779510 (-530.926132)	0.041387 (0.042607)	-531.120326 (-531.120653)	9.50 (9.50)	0.00 (0.00)
	3b	-531.779167 (-530.925199)	0.041524 (0.042659)	-531.119587 (-531.119886)	9.48 (9.48)	0.02 (0.02)
	3c	-531.774531 (-530.920602)	0.040717 (0.041968)	-531.114341 (-531.114653)	9.36 (9.36)	0.14 (0.14)
	3d	-531.774417 (-530.920203)	0.041119 (0.042249)	-531.114272 (-531.114534)	9.34 (9.34)	0.16 (0.16)

^a B3LYP/cc-pVTZ energy with zero-point energy correction in hartree.

^{a'} CCSD/cc-pVTZ energy with zero-point energy correction in hartree.

^b B3LYP/cc-pVTZ zero-point energy in hartree.

^{b'} CCSD/cc-pVTZ zero-point energy in hartree.

^c CCSD(T)/CBS energy in hartree (B3LYP/cc-pVTZ optimized geometry).

^{c'} CCSD(T)/CBS energy in hartree (CCSD/cc-pVTZ optimized geometry).

^d CCSD(T)/CBS ionization energy in eV with B3LYP/cc-pVTZ zero-point energy correction.

^{d'} CCSD(T)/CBS ionization energy in eV with CCSD/cc-pVTZ zero-point energy correction.

^e CCSD(T)/CBS relative energy in eV with B3LYP/cc-pVTZ zero-point energy correction.

^{e'} CCSD(T)/CBS relative energy in eV with CCSD/cc-pVTZ zero-point energy correction.

Table S5: Computed energies for the species related to the decomposition of phosphino formic acid (H_2PCOOH) and carbamic acid (H_2NCOOH).

Species	B3LYP/cc-pVTZ ^a (CCSD/cc-pVTZ ^{a'})	E_{zpc}^{b} ($E_{zpc}^{\text{b}'}$)	CCSD(T)/CBS ^c (CCSD(T)/CBS ^{c'})	$E(\text{kJ/mol})^{\text{d}}$ ($E(\text{kJ/mol})^{\text{d}'}$)
Phosphino formic acid 1a	-531.779440 (-530.925802)	0.041665 (0.042656)	-531.120540 (-531.120665)	51 (52)
Phosphino formic acid 1b	-531.771748 (-530.917714)	0.041360 (0.042377)	-531.112984 (-531.113136)	70 (71)
P-Transition state1	-531.762122 (-530.908825)	0.039894 (0.040945)	-531.102259 (-531.102381)	94 (95)
P-Transition state2	-531.707262 (-530.839762)	0.034742 (0.035725)	-531.035257 (-531.036070)	256 (256)
PH_3 and CO_2 complex	-531.805267 (-530.949533)	0.036169 (0.036709)	-531.135784 (-531.135945)	-4 (-4)
$\text{PH}_3 + \text{CO}_2$	-531.804993 (-530.948404)	0.035540 (0.036078)	-531.133704 (-531.133733)	0 (0)
Carbamic acid a	-245.193124	0.051062	-244.922591	10
Carbamic acid b	-245.181773	0.051052	-244.911794	38
N-Transition state 1	-245.177693	0.04996	-244.906250	50
N-Transition state 2	-245.128455	0.046209	-244.850349	187
NH_3 and CO_2 complex	-245.202530	0.047132	-244.926008	-10
$\text{NH}_3 + \text{CO}_2$	-245.199329	0.045965	-244.921192	0

^a B3LYP/cc-pVTZ energy with zero-point energy correction in hartree.

^{a'} CCSD/cc-pVTZ energy with zero-point energy correction in hartree.

^b B3LYP/cc-pVTZ zero-point energy in hartree.

^{b'} CCSD/cc-pVTZ zero-point energy in hartree.

^c CCSD(T)/CBS energy in hartree (B3LYP/cc-pVTZ optimized geometry).

^{c'} CCSD(T)/CBS energy in hartree (CCSD/cc-pVTZ optimized geometry).

^d CCSD(T)/CBS relative energy in kJ/mol with B3LYP/cc-pVTZ zero-point energy correction.

^{d'} CCSD(T)/CBS relative energy in kJ/mol with CCSD/cc-pVTZ zero-point energy correction.

References

1. B. M. Jones and R. I. Kaiser, *J. Phys. Chem. Lett.*, 2013, **4**, 1965-1971.
2. A. M. Turner, M. J. Abplanalp, S. Y. Chen, Y. T. Chen, A. H. Chang and R. I. Kaiser, *Phys. Chem. Chem. Phys.*, 2015, **17**, 27281-27291.
3. M. Bouilloud, N. Fray, Y. Benilan, H. Cottin, M. C. Gazeau and A. Jolly, *Mon. Not. Roy. Astron. Soc.*, 2015, **451**, 2145-2160.
4. D. Drouin, A. R. Couture, D. Joly, X. Tastet, V. Aimez and R. Gauvin, *Scanning*, 2007, **29**, 92-101.
5. M. Förstel, P. Maksyutenko, B. Jones, B.-J. Sun, A. Chang and R. Kaiser, *Chem. Commun.*, 2016, **52**, 741-744.
6. A. D. Becke, *J. Chem. Phys.*, 1992, **96**, 2155-2160.
7. A. D. Becke, *J. Chem. Phys.*, 1992, **97**, 9173-9177.
8. A. D. Becke, *J. Chem. Phys.*, 1993, **98**, 5648-5652.
9. C. Lee, W. Yang and R. G. Parr, *Phys. Rev. B*, 1988, **37**, 785.
10. M. J. Deegan and P. J. Knowles, *Chem. Phys. Lett.*, 1994, **227**, 321-326.
11. C. Hampel, K. A. Peterson and H.-J. Werner, *Chem. Phys. Lett.*, 1992, **190**, 1-12.
12. P. J. Knowles, C. Hampel and H. J. Werner, *J. Chem. Phys.*, 1993, **99**, 5219-5227.
13. G. D. Purvis III and R. J. Bartlett, *J. Chem. Phys.*, 1982, **76**, 1910-1918.
14. K. A. Peterson, D. E. Woon and T. H. Dunning Jr, *J. Chem. Phys.*, 1994, **100**, 7410-7415.
15. K. A. Peterson and T. H. Dunning Jr, *J. Chem. Phys.*, 1995, **99**, 3898-3901.
16. R. I. Kaiser, S. P. Krishtal, A. M. Mebel, O. Kostko and M. Ahmed, *Astrophys. J.*, 2012, **761**, 178.
17. M. J. Frisch, G. W. Trucks, H. B. Schlegel, G. E. Scuseria, M.A. Robb, J. R. Cheeseman, G. Scalmani, V. Barone, B. Mennucci, G. A. Petersson, H. Nakatsuji, M. Caricato, X. Li, H. P. Hratchian, A. F. Izmaylov, J. Bloino, G. Zheng, J. L. Sonnenberg, M. Hada, M. Ehara, K. Toyota, R. Fukuda, J. Hasegawa, M. Ishida, T. Nakajima, Y. Honda, O. Kitao, H. Nakai, T. Vreven, J. A. Montgomery, J. E. P. Jr., F. Ogliaro, M. Bearpark, J. J. Heyd, E. Brothers, K. N. Kudin, V. N. Staroverov, R. Kobayashi, J. Normand, K. Raghavachari, A. Rendell, J. C. Burant, S. S. Iyengar, J. Tomasi, M. Cossi, N. Rega, J. M. Millam, M. Klene, J. E. Knox, J. B. Cross, V. Bakken, C. Adamo, J. Jaramillo, R. Gomperts, R. E. Stratmann, O. Yazyev, A. J. Austin, R. Cammi, C. Pomelli, J. W. Ochterski, R. L. Martin, K. Morokuma, V. G. Zakrzewski, G. A. Voth, P. Salvador, J. J. Dannenberg, S. Dapprich, A. D. Daniels, Ö. Farkas, J. B. Foresman, J. V. Ortiz, J. Cioslowski and D. J. Fox, *Gaussian 09, Revision D. 01*, , Gaussian Inc., Wallingford CT, 2009.